Research Article

Thermal and mechanical performance of rigid polyurethane foam added with commercial nanoparticles

Caterina Lorusso[1], Viviana Vergaro[2,3], Francesca Conciauro[3],
Giuseppe Ciccarella[2,3] and Paolo Maria Congedo[1]

Abstract

This study investigates the effects of commercial nanoparticles on thermal and mechanical performance of rigid poly-urethane foams. Two different types of nanoparticles are considered as fillers, spherical titania and rod-shaped halloysite clay nanotubes. The aim of this study was to produce rigid polyurethane foams modified with titania nanocrystals and nanohalloysite in order to obtain polyurethanes with improved properties. The laboratory scale-up will be suitable for the production in many branches of industry, such as construction and automotive production. In particular, these foams, added with commercial nanoparticles, characterized by better thermal and mechanical properties, are mainly used in construction for thermal insulation of buildings. The fillers were dispersed in the components, bringing rates up to 10%. In these investigations, the improvement of the thermal properties occurs by adding nanoparticles in the range 4–8% of titania and halloysite. The mechanical properties instead have been observed an improvement starting from 6% of nanoparticles addition. All data are in agreement with scanning electron microscope observations that shown a decrease in the average cell size and an increase in the cell density by adding nanoparticles in foams.

Introduction

The foams optimized with nanoparticles exhibit increased strength and damping properties over traditional foams.[1–10] Foams added with nanoparticles are defined as composites with a polymer matrix and fillers that are less than 100 nm in at least one dimension. The nanoparticles offer a convenient opportunity in the formation of polymer foams for several key reasons[2]: to function as heterogeneous nucleation sites; to provide conductivity or mechanical strength of the foam while not decreasing other properties; to change the rheological properties; to reduce the energy for bubble nucleation; and to change the structure and density of the foam.

Therefore, the use of nanoparticles may lead to a sensible variation of foam morphology, with an enhancement of thermal insulating properties, a reduction of the thermal aging phenomena and an enhancement of the mechanical properties.[1–10]

[1] Department of Engineering for Innovation, University of Salento, Lecce, Italy
[2] Biological and Environmental Sciences Department, University of Salento, Lecce, Italy
[3] CNR NANOTEC – Institute of Nanotechnology c/o Campus Ecotekne, University of Salento, Lecce, Italy

Corresponding Authors:
Caterina Lorusso and Paolo Maria Congedo, Department of Engineering for Innovation, University of Salento, via Monteroni, Lecce I-73100, Italy.
Emails: caterina.lorusso@unisalento.it; paolo.congedo@unisalento.it

Standard polyurethane (PU) foams have some limitations, such as low mechanical strength and low thermal stability.[1,2] The properties of PU depend not only on the intrinsic properties of the raw materials but also on the foam morphology, such as cell density, cell size and size distribution. Therefore, one of the most important aspects of PU research is to enhance the strength of the foam without compromising its lightweight. There are two approaches to solve this issue. The first one is to decrease the average cell size without decreasing the foam density, meant as the final bulk density of the product. The second approach is to use fillers to reinforce the polymer matrix. A special interest is addressed in the use of nanofillers to decrease cell size and at the same time to reinforce the polymeric matrix.

In very recent works,[11–13] materials for the building containing synthesized nanoparticles have been tested in the laboratory, and the improved properties were attributed to surface treatments of nanofillers. In this work, some commercial nanoparticles have been employed in building sites due to their low cost, instead of those synthesized in the laboratory. The originality of this work is due to the choice of the nanoparticles. The titania (TiO_2) has been used for its particular property of absorbing the solar radiation. In this way, the TiO_2 becomes reactive and allows oxygen to react with the organic substances dangerous for humans, transforming them into the anhydrite carbon dioxide and water. Since the shape of the TiO_2 is spherical, it has been decided to put it in comparison with a commercial elongated nanoparticle such as halloysite. Halloysite clay nanotubes (HNTs) have two dimensions at the nanometric scale while the third is larger, these particles possess an elongated structure. TiO_2 nanoparticles have all three dimensions at the nanometric scale.

This choice has been due to the previous work[12] in which the behaviour of elongated nanoparticles is better than the spherical shape ones, but this effect is still under investigation.

Cell size, size distribution and cell density depend on the cell nucleation and cell growth mechanisms, all of which contribute to the final bulk density of the product. The cell size is inversely proportional to the number of nucleation sites, and the percentage of nanofillers can increase the nucleation rate[14–26]; for this reason, in this work, we have used the percentage of filler up to 10%. An improvement of thermal and mechanical properties has been reached, and these results have been compared with morphological analyses performed with scanning electron microscopy (SEM).

Materials and methods

Raw materials

The main components for a PU foam are as follows: polyols (Varanol RH 360, CP 260, Dow Chemical Company,

Table 1. Foam formulations and densities.[12]

Formulation	Sample
Voranate M 600 (g)	165
Varanol RH360 (g)	90
CP 260 (g)	10
Polycat 5 (g)	0.15
Polycat 8 (g)	2.7
Tegostab B 8496 (g)	2.5
Water (g)	2.4
Cyclopentane (g)	9
Density (g/l)	36.1

Italy) and the isocyanate (Voranate M 600, Dow Chemical Company, Italy). In the foam formulation, a primary polyol and a secondary polyol were used. The characteristic of the primary polyol (Varanol RH 360, Dow Chemical Company, Carpi, Correggio, Italy) is of having many hydroxyl groups, while the secondary polyol (CP 260, Dow Chemical Company, Carpi, Correggio, Italy) promotes the reaction. The contribution of CP 260 must remain low, because it causes an opening of the cells. The isocyanate is very reactive towards components that have active hydrogen (polyols). As regards the preparation of rigid foams, it has been considered appropriate to use an oligomeric diphenylmethane diisocyanate. The kinetics of polymerization have been favoured adding the catalysts supplied with Air Product (Polycat 5 and Polycat 8, Dow Chemical Company, Italy). Among the physical foaming agents, cyclopentane has been chosen (provided by Sigma Aldrich, Milan, Italy) for its good solubility in the polymer matrix and low thermal conductivity. These characteristics led to the production of the PU with good insulation and physical properties.

To improve the stability and the cellular regulation, the polyol mixture has been added to a silicon reagent (copolymer polyester–polysiloxane) provided by Evonik: Tegostab B 8474.

The particles introduced are commercial purified dehydrated HNTs, obtained from Applied Minerals, Inc. (New York City, New York, USA), and Aeroxide TiO_2 (P25) nanocrystals chosen for its characteristic of being inexpensive and non-toxic.[27] P25 nanocrystals are a commercial product made by pyrolysis and consist of 80% of anatase crystal phase and 20% of rutile.

Foam formulations and densities are reported in Table 1.

Foam preparation

The rectangular panels have been realized through the foaming in batch and are accomplished by pouring the reaction mixture into a plastic mould of size 400 × 400 × 40 mm (Figure 1). The mould is coated with an aluminium sheet of thickness 1 mm, to avoid the reaction between the plastic mould and the reagents of the reaction mixture.
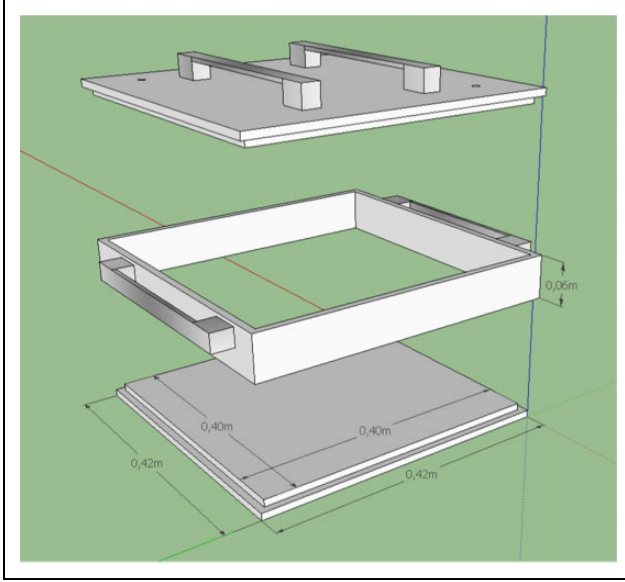
Figure 1. Mould for foaming.

The mould is designed to resist to an internal pressure of 2–3 bar; there are three holes to allow the evacuation of the gases, produced during the foaming. The nanoparticles have been dispersed using an UltraTurrax DI 18 Basic, with speed 23,000 r/min for 1 h. This period has been needed to not overheat the mixture and to have a good dispersion of the nanoparticles. In the preparation of PU, the amount of each reagent must meet strict stoichiometric ratios. After having established the grams of polyols (100 g), to determine the right amount of isocyanate to use, it is necessary to ensure that the isocyanate groups –NCO react only with a hydroxyl group –OH. The number of hydroxyl n_{OH} is[28]

$$n_{OH} = \frac{56,100 \times f}{MW} \quad (1)$$

where f is the functionality and MW is the molecular weight. The equivalent weight in gram per mole is defined by

$$W_{eq} = \frac{MW}{f} \quad (2)$$

Replacing equation (1) in (2), the equivalent weight of the hydroxyl groups is obtained

$$W_{eq,OH} = \frac{56,100}{n_{OH}} \quad (3)$$

Similarly, the equivalent weight of the isocyanate groups can be obtained

$$W_{eq, NCO} = \frac{42}{\%NCO} \quad (4)$$

where %NCO is the concentration of the –NCO group reactive in the isocyanate compared to the weight. The number of equivalent (n_{eq}) can be defined by

$$n_{eq} = \frac{g}{W_{eq}} \quad (5)$$

where g is the weight in grams. The grams of isocyanate are

$$g_{NCO} = n_{eq} \times W_{eq,NCO} \quad (6)$$

As already mentioned, the isocyanate groups react by following a unitary relationship with the hydroxyl groups. Therefore, it is better expressed using equation (4) in terms of the equivalent of hydroxyl. It refers to a weight of 100 g and employing equation (4), equation (6) becomes

$$g_{NCO} = \frac{100 \, g_{OH}}{W_{eq,OH}} \times \frac{42}{\%NCO} \quad (7)$$

Using equation (4), we obtain

$$g_{NCO} = \frac{n_{OH}}{NCO} \times 7.5 \quad (8)$$

Operating with a mixture of polyols with different hydroxyl numbers and considering the chemical agent water, the n_{OH} of equation (8) is the weighted average of all hydroxyl numbers, and for this, equation (8) becomes

$$g_{NCO} = \left(\frac{g_{pol1}}{100} \times n_{OH_1} + \frac{g_{pol2}}{100} \times n_{OH_2} + \cdots + \frac{g_{H_2O}}{100} \times n_{OH_{H_2O}} \right) \\ \times \frac{7.5}{\%NCO} \quad (9)$$

Equation (9) is used to calculate the grams of isocyanate. In this equation, not only the hydroxyl groups are taken into account but also all the polyols put in the mixture, including water –OH, where $n_{OH_{H_2O}}$ is 6220 mg KOH/g. The real quantity of isocyanate used differs from the stoichiometric one: It generally needs a greater quantity to ensure the complete reaction of polyols. The quantity that really is used is expressed by the following relationship

$$I = \frac{\text{real quantity of isocyanate}}{\text{stoichiometric quantity of isocyanate}} \times 100 \quad (10)$$

Practically, this index has been set equal to 1.1 ÷ 1.3; in fact, if a greater index had been used, what would result is an excess of reactive isocyanate with a consequent worsening of the mechanical properties.

For the amount of blowing agent used, it is necessary to apply an appropriate equation. It is known that putting an excessive amount of blowing agent compared to the theoretical value obtained, it will have negative consequences on the structure of the foam that will be less thick and very porous with disastrous results both on the mechanical properties and on the thermal conductivity. In fact, minimum values of conductivity are obtained for a density ranging between 30 and 40 kg/m³; if they differ from these values, the conductivity increases.

The mass of blowing agent (cyclopentane and water**)** to add has been calculated in this way[28]

$$\rho = \frac{m_{tot}}{V} = \frac{m_{PU} + m_{BA}}{V_0 \left(\frac{m_{BA}}{WM_{BA}} + \frac{m_{H_2O}}{WM_{H_2O}} \right) \times \frac{T}{T_0}} \quad (11)$$

where m_{PU} is the mass PU, while m_{BA} is the mass of blowing agent. The volume V can be approximated to that of the

expanding gas, because the foam is made to 97% by gas. Usually, the value assigned to the ratio T/T_0 is included in the range $1.3 \div 1.6$.

The WM_{H_2O} is 18 kg/m³, while the WM_{BA} is 150 kg/m³. The mass of blowing agent is obtained by the following equation

$$m_{BA} = \frac{m - \left(V_0 \times \frac{T}{T_0} \times \frac{m_{H_2O}}{WM_{H_2O}} \times \rho\right)}{\frac{V_0}{WM_{BA}} \times \frac{T}{T_0} \times \rho - 1} \qquad (12)$$

It has been noticed that although equation (12) has been applied and then employed the precise amount of blowing agent, the density result was not coincident to the real.

It is very important to calculate the amount of foaming agents, particularly water, because the residual water makes even more difficult to control the density of the final material. This probably depends on the interactions that the different types of nanoparticles have with water.

Morphological analysis

The morphology of the foams has been studied by means of SEM (Carl Zeiss Merlin, Jena, Germany). The material has been cut with a razor blade, and the fracture surface was sputter-coated with gold before observation; the accelerating voltage is set at 5 kV to avoid degradation of the sample. The morphological characterization has been used to study the filler dispersion and the mean cell size. The cell density (N_f) was calculated according to equation (13) and then normalized to the ratio between the nanocomposite foam density and the neat PU foam cells[19–21]

$$N_f = \left(\frac{nM^2}{A}\right)^{3/2} \qquad (13)$$

where n is the number of cells, A is the area in a SEM micrograph and M is the magnification factor.

Thermal conductivity measurements

Thermal conductivity measurements of PUs are obtained using a transient technique called hot disc experiment. The Hot Disk Thermal Constants Analyzer (Göteborg, Sweden) is a system designed to measure the thermal transport properties of a sample: thermal conductivity, thermal diffusivity and specific heat. The system is based on a patented transient plane source technique that follows DIN EN ISO 22007-2; it can be used to study materials with thermal conductivities from 0.005 W/m K to 500 W/m K and covering a temperature range from 30 K to 1000 K. The reproducibility of the instrument is typically better than 1%, and the accuracy is better than 5%. The measurements have been carried out according to UNI EN 13165[29], and the analysis procedure of the Hot Disk was reported in the following documents.[30,31] The predefined shape of the sample is not important; it is essential that the sample has

a flat surface in each of the two halves, which has been obtained from the band saw, and has been thermostated for 24 h at 23°C. During the measure, the temperature follows a transitory with an increase of around 0.5°C above the temperature environment.

Physical–mechanical properties

The tests have been made on specimens of prismatic side with square base, with a nominal thickness of 25 mm and a relative error within 0.5%, according to the UNI EN 826,[32] due to the cut of the band saw, with which the tests have been cut. The width of the specimens must not be less than their thickness in order not to reduce the accuracy of the result. It has been applied a load of 250 Pa and press the sample at a constant crosshead speed with a servo-hydraulic TECNOTEST testing system. The machine for compression test provided two parallel smooth plates of steel, having at least the diameter equal to the side of the specimen under test. One of the plates has been fixed, but having the possibility to move with a constant speed, while the other is movable, consisting of a ball joint positioned centrally, so as to ensure that the specimen is subjected exclusively an axial force. The machine consists of a device for the measurement of the displacement and a sensor fixed to one of the plates to measure the force produced by the reaction of the specimen on the plates. For PUs when the stress maximum corresponds to a deformation lower than 10%, it is defined 'compressive strength'.

The specimens have been conditioned for at least 6 h at 23 ($\pm$ 5)°C, and the test has been conducted at 23 ($\pm$ 5)°C. The placing of the specimens occurs between the parallel plates of the machine for the compression test; it is very important that the base of the specimen is normal to the direction of compression and that has been applied a preload of 250 ($\pm$ 10) Pa. The specimen was compressed with the mobile plate set at a constant speed of 2.5 mm/min, and the test continued until reaching a deformation of 10%.

Results and discussion

Morphological characterization

When a filler is introduced into a polymeric material, the ideal is to have a regular granulometry and that its particles are sufficiently small to enable better distribution in the matrix. Figure 2 presents the image obtained with transmission electron microscopy of commercial TiO_2 Aeroxide P25 and SEM of commercial HNTs.

Nanoparticles act as nucleation agents and promote the cell nucleation because of an effective decrease in the required energy for creating bubbles. According to the 'classical' theory of homogeneous nucleation, the formation of a gas bubble in a liquid mass is associated with a change in Gibbs free energy. The free energy expression of
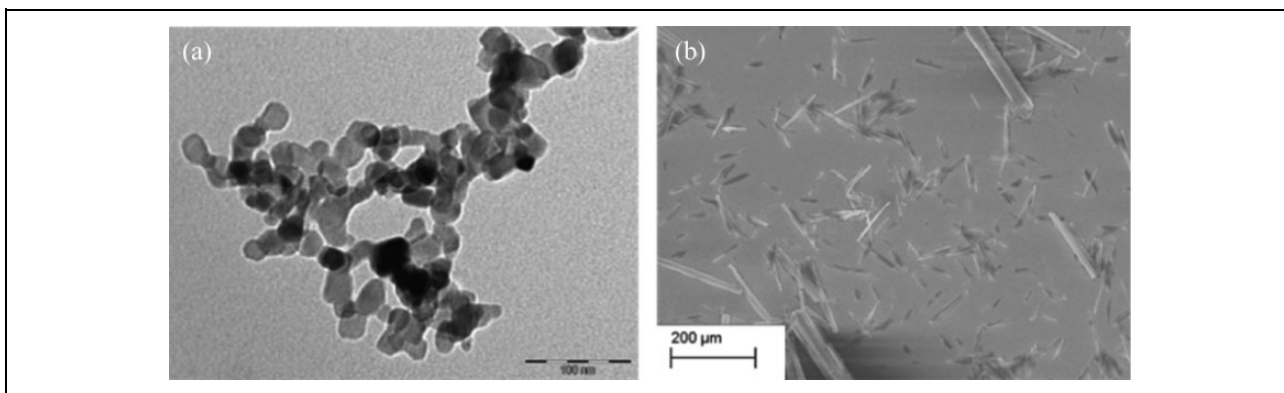
Figure 2. (a) TEM image of TiO_2 Aeroxide P25. (b) SEM image of HNTs. TEM: transmission electron microscopy; SEM: scanning electron microscopy; HNTs: halloysite clay nanotubes; TiO_2: titania.

Gibbs has a maximum point in correspondence with the critical radius R_c value. For values of radius less than R_c, the bubbles formed tend to dissolve again into the liquid. Their growth, in fact, is thermodynamically a disadvantage, since it requires an increase in free energy. For higher values of radius R_c, the bubble tends to grow, because this growth corresponds to a decrease in free energy.

Any solid element introduced into the mixture, such as nanoparticles, tends to decrease the value of ΔG and thus promote the nucleation. When the nucleation occurs near the interface with a third phase, generally solid, it is called heterogeneous nucleation.

The energy barrier for the heterogeneous nucleation is much reduced compared to the homogeneous one; in particular, the higher the solid–liquid surface tension and the lower the bubble–solid surface tension, the more it decreases. In this study, there has been a higher nucleation in the case of halloysite, carrying out an improved thermal conductivity, due to the higher solid–liquid surface tension.

Nanoparticles in comparison with conventional nucleating agents have a very extensive surface contact with the polymer matrix and very high surface density. Compared to conventional micron-sized filler particles used in the foaming processes, nanoparticles offer unique advantages for enhanced nucleation. The improved nucleation efficiency is reported in many studies for different polymer/nanoparticle systems at very low particle content rations.[4,17,33–42]

The extremely fine dimensions and large surface area of nanoparticles provide a more intimate contact between the particles, polymer matrix and gas. Probably, the rod shape of halloysite, compared to the spherical shape of TiO_2, constitutes a major impediment in the mixture of the liquid that will generate the PU foam. As it has been mentioned earlier, every obstacle it contributes lowers the Gibbs free energy by promoting the nucleation, thereby increasing the insulating properties.

Furthermore, a significantly higher effective particle concentration can be achieved at a low nominal particle concentration.
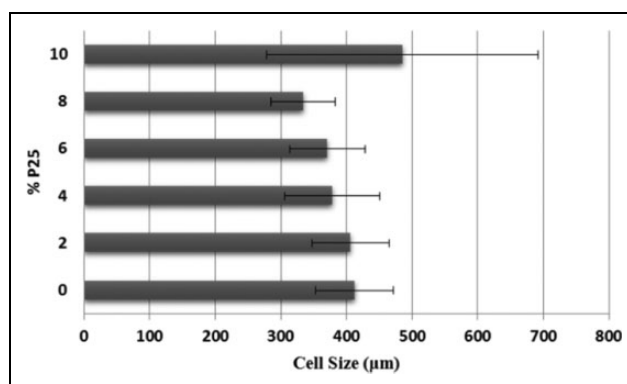

Figure 3. Cell size (μm) of polyurethane foam additivated with TiO_2 P25 nanoparticles. TiO_2: titania.
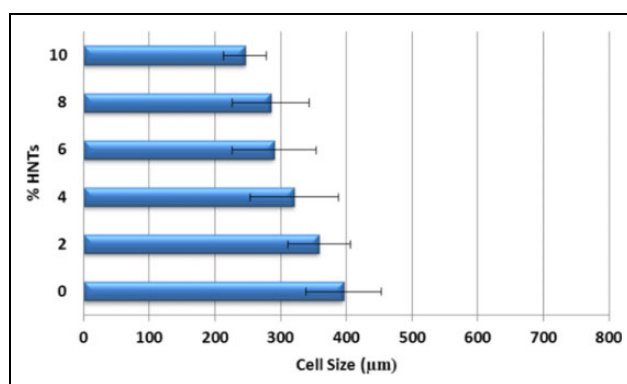

Figure 4. Cell size (μm) of polyurethane foam additivated with HNTs nanoparticles. HNTs: halloysite clay nanotubes.

The morphology of nanocomposite foams was evaluated by SEM (AIS-2100, Seron Technology, Korea). The foam mean cell size (Figures 3 and 4) has been measured by ImageJ (autocad autodesk) software, and the values have been obtained as an average of minimum 200 cells; the cell density (Table 1) was calculated from SEM micrographs. By analysing foams morphology in detail, it has been shown that the filler dispersion has been always fairly

Table 2. Wall thickness (nm) and density (N_f) (cells/cm^3) of pure foam (neat) and nanoreinforced foams with TiO$_2$ P25 and HNTs.

Type	Wall thickness (nm) (mean $\pm$ SD)	Cell density (N_f) (mean $\pm$ SD)
Neat PU foam	395 $\pm$ 6.22	5.00 $\pm$ 0.36
TiO$_2$ 2%	401.2 $\pm$ 5.3	4.97 $\pm$ 0.43
TiO$_2$ 4%	410.0 $\pm$ 2.5	5.13 $\pm$ 0.60
TiO$_2$ 6%	430.3 $\pm$ 4.4	5.15 $\pm$ 0.64
TiO$_2$ 8%	450.4 $\pm$ 1.5	5.18 $\pm$ 0.69
TiO$_2$ 10%	371.3 $\pm$ 9.7	5.07 $\pm$ 0.82
HNTs 2%	402.1 $\pm$ 5.2	5.05 $\pm$ 0.43
HNTs 4%	412.7 $\pm$ 4.7	5.18 $\pm$ 0.60
HNTs 6%	416.4 $\pm$ 7.4	5.22 $\pm$ 0.64
HNTs 8%	491.5 $\pm$ 4.1	5.26 $\pm$ 0.70
HNTs 10%	343.1 $\pm$ 7.8	5.36 $\pm$ 0.82

HNTs: halloysite clay nanotubes; TiO$_2$: titania.

good: No agglomeration of great dimensions can be found.

All foams exhibit polygons closed-cell structures with energetically stable pentagonal and hexagonal faces. The neat PU foam has fewer cells and a larger cell size than PU nanocomposite foams. From SEM images, the cell size, wall thickness and density were measured and summarized in Table 2. From the figure, it can be seen that the cell size is different for the pure PU foam and the nanoreinforced foam. PU foams containing nanoparticles have a higher cell density N_c and smaller cell size d, suggesting that the dispersed nanoparticles act as heterogeneous nucleation sites during cell formation. With the addition of nanoparticles, the overall cell structure has become less uniform, the cell walls have become thicker, and there is a larger amount of broken cells, above all in the samples prepared adding 10% of nanoparticles, in which, also, a decrease in cell walls has been observed.

Alterations in the cell morphology are due to the presence of nanoparticles that affect the process of cell nucleation.

In general, a decrease in the cell size of the foam containing nanoparticles is due to nanoparticles serving as nucleation points, resulting in the formation of a larger number of cells and, hence, a smaller cell size. Thus, the key issues in decreasing the cell size and increasing the cell density are addition of small amounts of nanoparticles and their uniform dispersion within the matrix material.

Figure 5 shows SEM images of the fractured surface of PU foams.

Thermal conductivity

The results on thermal conductivity of the neat, TiO$_2$ and HNTs nanoadditivated PUs are summarized in Table 3. The TiO$_2$ additived foams show the same trend of the conductivity value 3 and 10 days after production. The data of thermal conductivity are worsening up 6%,
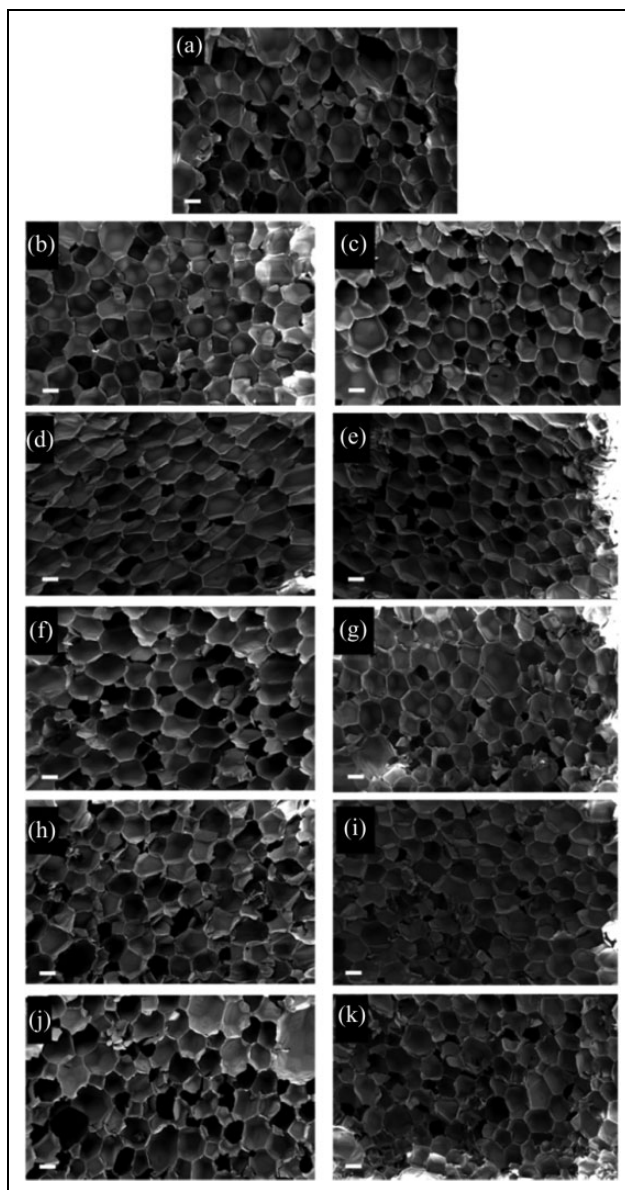

Figure 5. (a) Neat foam; nanoreinforced polyurethane foams: (b, c) P25–HNTs 2%; (d, e) P25–HNTs 4%; (f, g) P25–HNTs 6%; (h, i) P25–HNTs 8%; (j, k) P25–HNTs 10%. Scale bar 200 μm. HNTs: halloysite clay nanotubes.

probably, because the nanoparticles have been badly dispersed in the mixture generating a conductivity value unstable.

This is due to two factors: the first one is that the agglomerates arranged on the wall (Table 2) rather than at the nodes of the cell and the second one is the presence of many broken cells.

PU foams additivated with HNTs after 3 days from the production, the conductivity value continues to decrease gradually with increasing percentage of nanoparticles until 8%.

For both foam compositions, when the nanoparticles concentration reaches 10%, detrimental effects in terms

Table 3. Thermal conductivity – HNTs and TiO$_2$.

Type	Thermal conductivity (W/m K) 3 days after (mean value $\pm$ SD)	Thermal conductivity (W/m K) 10 days after (mean value $\pm$ SD)
Neat PU foam	0.0254 $\pm$ 0.0006	0.0262 $\pm$ 0.0003
TiO$_2$ 2%	0.0246 $\pm$ 0.0003	0.0249 $\pm$ 0.0003
TiO$_2$ 4%	0.0244 $\pm$ 0.0007	0.0261 $\pm$ 0.0006
TiO$_2$ 6%	0.0292 $\pm$ 0.0015	0.0342 $\pm$ 0.0003
TiO$_2$ 8%	0.0254 $\pm$ 0.0001	0.0262 $\pm$ 0.0005
TiO$_2$ 10%	0.0329 $\pm$ 0.0007	0.0343 $\pm$ 0.0003
HNTs 2%	0.0263 $\pm$ 0.0018	0.0263 $\pm$ 0.0003
HNTs 4%	0.0242 $\pm$ 0.0004	0.0309 $\pm$ 0.0008
HNTs 6%	0.0239 $\pm$ 0.0001	0.0262 $\pm$ 0.0002
HNTs 8%	0.0236 $\pm$ 0.0001	0.0262 $\pm$ 0.0005
HNTs 10%	0.0245 $\pm$ 0.0009	0.0343 $\pm$ 0.0003

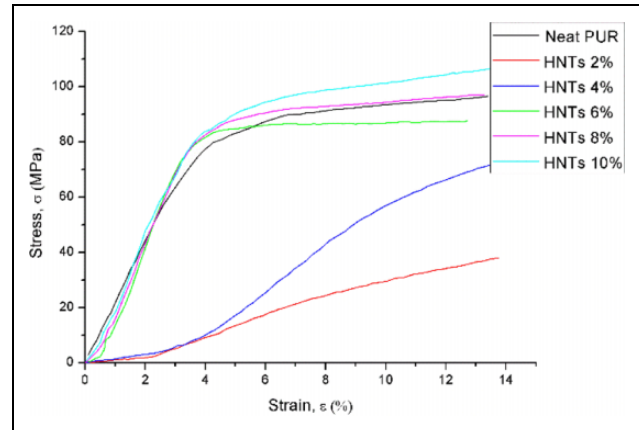HNTs: halloysite clay nanotubes; TiO$_2$: titania.
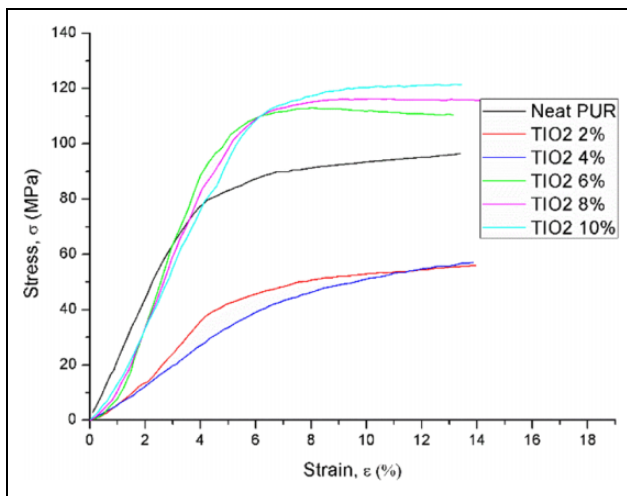
Figure 6. Compression stress–strain plot TiO$_2$. TiO$_2$: titania.

of conductivity happened. The addition of nanoparticles, above 8%, leads to the formation of some bigger and some broken that deprives the foam of its insulating properties.

Physical–mechanical testing

Compressive stress–strain curves for the neat and nanophased PU foams are shown in Figures 6 and 7.

The curves show three stages of deformation: initial linear behaviour, linear plateau region and densification. The initial slope is used to calculate the compressive modulus of foam, and the intersection point between the initial slope and the plateau slope is used to calculate the compressive strength. In Figure 6, it is observed that the compressive modulus and strength are higher, of foams added with 6, 8 and 10% of TiO$_2$, than the neat. For low dispersions, 2–4%, TiO$_2$ PU foam shows lower values than the neat. Moreover, the low slope depends and the shape of the plateau region depends on the morphology of cells. In case of linear plateau, cell deformation occurs as combination of

Figure 7. Compression stress–strain plot HNTs. HNTs: halloysite clay nanotubes.

cell bending and collapse. Thus, it can be said that the behaviour of the PU foam can be improved due to infusion of nanoparticles.

In Figure 7, the curve of the neat foam has a trend similar to the additivated foams with 6, 8 and 10%, while the foams, added in 2 and 4%, suffer strong deformations with applications of small loads, so these foams are not able to be used in zones of the buildings designed to trampling. The results of compression tests show that infusion of HNTs gives more strength to the cells.

Conclusions

The nanoreinforced PU foams manufactured with two different types of nanoparticles, TiO$_2$ (Aeroxide P25) and HNTs, have been dispersed into the PU matrix through sonication technique. Both neat and nanophased foams are tested in compression and thermal analysis. The microstructure has been investigated by the SEM. It is observed that PU/TiO$_2$ shows the highest performance for mechanical properties, because of the infusion of TiO$_2$, which gives more strength to the cells. Probably, as the nanoparticles are arranged on the walls of the cells, it generates an increase in the wall thickness that confers a higher mechanical resistance. PU/HNTs shows, instead, the highest performance for thermal properties in terms of thermal conductivity immediately after production, showing a continuous decrease in the conductivity values in inverse proportion to the addition of nanoparticles up to 8%. As reported in the literature, the improvement of thermal and mechanical properties has been obtained using elongated nanoparticles, such as clays or carbon nanotubes.[5] For this reason, it has been decided to compare halloysite with spherical nanoparticles (TiO$_2$) for testing if rising the percentage (up to 10%) of fillers confers an enhancement of foam properties. The results show that despite the high percentage of fillers, the behaviour of elongated nanoparticles is better than the spherical ones. Probably, the elongated shape of the nanoparticles makes the energy of

nucleation decrease much more, with respect to the spherical shape, by making the number of nucleation to increase. This structure ensures the presence of gas inside the cells, which gives better insulating properties. All data are confirmed by the SEM analysis. The literature is full of novel nanocomposite materials; but in order to move these materials into commercial products, several challenges must be overcome. For future developments, we could combine nanoparticles with different shapes, with high surface area and rich surface chemistry[12] trying to optimize the production protocol. If these improvements have been due to the different shapes of nanoparticles or by surface treatments,[1] this can be confirmed by further studies.

Acknowledgements

Declaration of conflicting interests

Funding

References

1. Lee LJ, Zeng C, Cao X, et al. Polymer nanocomposite foams. *Compos Sci Technol* 2005; 65(15–16): 2344–2363.

2. Chen L, Rende D, Schadler LS, et al. Polymer nanocomposite foams. *J Mater Chem* 2013; 1(12): 3837–3850.

3. Widya T and Macosko CW. Nanoclay-modified rigid polyurethane foam. *J Macromol Sci* 2005; 44(6): 897–908.

4. Bahrambeygi H, Rabbi A, Nasouri K, et al. Morphological and structural developments in nanoparticles polyurethane foam nanocomposite's synthesis and their effects on mechanical properties. *Adv Polym Tech* 2013; 32(S1): E545–E555.

5. Saha MC, Kabir ME and Jeelani S. Enhancement in thermal and mechanical properties of polyurethane foam infused with nanoparticles. *Mater Sci Eng: A* 2008; 479(1–2): 213–222.

6. Kim H and Macosko CW. Morphology and properties of polyester/exfoliated graphite nanocomposites. *Macromolecules* 2008; 41(9): 3317–3327.

7. Shafi MA, Joshi K and Flumerfelt RW. Bubble size distributions in freely expanded polymer foams. *Chem Eng Sci* 1997; 52(4): 635–644.

8. Modesti M, Lorenzetti A and Besco S. Influence of nanofillers on thermal insulating properties of polyurethane nanocomposites foams. *Polym Eng Sci* 2007; 47(9): 1351–1358.

9. Chen L, Ozisik R and Schadler LS. The influence of carbon nanotube aspect ratio on the foam morphology of MWNT/PMMA nanocomposite foams. *Polymer (Guilford)* 2010; 51(11): 2368–2375.

10. Dolomanova V. Mechanical properties and morphology of nano-reinforced rigid PU foam. *J Cell Plast* 2011; 47(1): 81–93.

11. Carlucci C, Conciauro F, Scremin BF, et al. Properties of aluminosilicate refractories with synthesized boron-modified TiO_2 nanocrystals. *Nanomaterials and Nanotechnology* 2015; 5. DOI: 10.5772/60204.

12. Lorusso C, Vergaro V, Monteduro A, et al. Characterization of polyurethane foam added with synthesized acetic and oleic-modified TiO_2 nanocrystals. *Nanomaterials and Nanotechnology* 2015; 5: 1–7. DOI: 10.5772/61275.

13. Conciauro F, Filippo E, Carlucci C, et al. Properties of nanocrystals-formulated aluminosilicate bricks. *Nanomaterials and Nanotechnology* 2015; 5: 28. DOI: 10.5772/61068.

14. Feng JJ and Bertelo CA. Prediction of bubble growth and size distribution in polymer foaming based on a new heterogeneous nucleation model. *J Rheol* 2004; 48(2): 439–462.

15. Goren K, Chen L, Schadler LS, et al. Influence of nanoparticle surface chemistry and size on supercritical carbon dioxide processed nanocomposite foam morphology. *J Supercrit Fluids* 2010; 51(3): 420–427.

16. Yeh JM, Chang KC, Peng CW, et al. Preparation and insulation property studies of thermoplastic PMMA-silica nanocomposite foams. *Polym Compos* 2009; 30(6): 715–722.

17. Zeng C, Han X, Lee LJ, et al. Polymer-clay nanocomposite foams prepared using carbon dioxide. *Adv Mater* 2003; 15(20): 1743–1747.

18. Siripurapu S, DeSimone JM, Khan SA, et al. Controlled foaming of polymer films through restricted surface diffusion and the addition of nanosilica particles or CO 2-philic surfactants. *Macromolecules* 2005; 38(6): 2271–2280.

19. Zeng C, Hossieny N, Zhang C, et al. Synthesis and processing of PMMA carbon nanotube nanocomposite foams. *Polymer* 2010; 51(3): 655–664.

20. Chang Y-W, Lee D and Bae S-Y. Preparation of polyethylene-octene elastomer/clay nanocomposite and microcellular foam processed in supercritical carbon dioxide. *Polym Int* 2006; 55(2): 184–189.

21. Zhu B, Zha W, Yang J, et al. Layered-silicate based polystyrene nanocomposite microcellular foam using supercritical carbon dioxide as blowing agent. *Polymer* 2010; 51(10): 2177–2184.

22. Wee D, Seong DG and Youn JR. Processing of microcellular nanocomposite foams by using a supercritical fluid. *Fibers and Polym* 2004; 5(2): 160–169.

23. Guo Z, Lee LJ and Tomasko DL. CO_2 permeability of polystyrene nanocomposites and nanocomposite foams. *Ind Eng Chem Res* 2008; 47(23): 9636–9643.

24. Yang J, Wu M, Chen F, et al. Preparation, characterization, and supercritical carbon dioxide foaming of polystyrene/

graphene oxide composites. *J Supercrit Fluids* 2011; 56(2): 201–207.

25. Zhai W. Heterogeneous nucleation uniformizing cell size distribution in microcellular nanocomposites foams. *Polymer (Guilford)* 2006; 47(21): 7580–7589.

26. Chang Y-W, Kim S, Kang SC, et al. Thermomechanical properties of ethylene-propylene-diene terpolymer/organoclay nanocomposites and foam processing in supercritical carbon dioxide. *Korean J Chem Eng* 2011; 28(8): 1779–1784.

27. Vergaro V, Abdullayev E, Lvov YM, et al. Cytocompatibility and uptake of halloysite clay nanotubes. *Biomacromolecules* 2010; 11(3): 820–826.

28. Randall D and Lee S. *The polyurethanes book*. New York: Wiley & Sons Ltd., 2002.

29. UNI EN 13165: 2006 Thermal insulation products for buildings – Factory made rigid polyurethane foam (PU) products.

30. He Y. Rapid thermal conductivity measurement with a hot disk sensor: Part 1. Theoretical considerations. *Thermochim Acta* 2005; 436(1–2): 122–129.

31. Instruction Manual. Hot Disk Thermal Constants Analyser Windows 95/98 Version 5.0. Hot Disk AB: Uppsala, Sweden, 1999.

32. UNI EN 826: 1998 Thermal insulating products for building applications – Determination of compression behavior.

33. Zhu J, Kim J, Peng H, et al. Improving the dispersion and integration of single-walled carbon nanotubes in epoxy composites through functionalization. *Nano Lett* 2003; 3(8): 1107–1113.

34. Nam PH, Maiti P, Okamoto M, et al. Foam processing and cellular structure of polypropylene/clay nanocomposites. *Polym Eng Sci* 2002; 42(9): 1907–1918.

35. Strauss W and Souza NAD. Supercritical CO_2 processed polystyrene nanocomposite foams. *J Cellular Plast* 2004; 40(3): 229–241.

36. Han X, Zeng C, Lee LJ, et al. Extrusion of polystyrene nanocomposite foams with supercritical CO_2. *Polym Eng Sci* 2003; 43(6): 1261–1275.

37. Sinha Ray S and Okamoto M. New polylactide/layered silicate nanocomposites, 6. *Macromol Mater Eng*, 2003; 288(12): 936–944.

38. Di Y, Iannace S, Di Maio E, et al. Poly(lactic acid)/organoclay nanocomposites: thermal, rheological properties and foam processing. *J Polym Science, Part B: Polym Phys* 2005; 43(6): 689–698.

39. Mitsunaga M, Ito Y, Ray SS, et al. Intercalated polycarbonate/clay nanocomposites: nanostructure control and foam processing. *Macromol Mater Eng* 2003; 288(7): 543–548.

40. Cao X, James Lee L, Widya T, et al. Polyurethane/clay nanocomposites foams: processing, structure and properties. *Polymer* 2005; 46(3): 775–783.

41. Shen J and Lee LJ. *Effects of carbon nanofibers on polystyrene nanocomposites and foams*. In: *62nd Annual technical conference – Society of Plastics Engineers* 2004; 2: 1836–1840.

42. Lee MH, Lee B and Choi K. Polyvinyl chloride foams - US Patent App. 10/546,299, 2004.